Sensors & Actuators: B. Chemical 306 (2020) 127564

Contents lists available at ScienceDirect

Sensors and Actuators B: Chemical

journal homepage: www.elsevier.com/locate/snb

Visual detection of lead ions based on nanoparticle-amplified magnetophoresis and Mie scattering

Lok Ting Chu[a], Hoi Man Leung[b], Pik Kwan Lo[b], Ting-Hsuan Chen[a,*]

[a] Department of Biomedical Engineering, City University of Hong Kong, Hong Kong Special Administrative Region
[b] Department of Chemistry, City University of Hong Kong, Hong Kong Special Administrative Region

ARTICLE INFO

Keywords:
Visual detection
Lead ion
DNAzyme
Nanoparticles

ABSTRACT

Lead poisoning in drinking water is a serious threat to public health as it may cause permanent damage to the human nervous system and developmental disorders in children. Many detection methods were developed based on fluorometric, electrochemical, and chemiluminescent assays, but they require precise instruments for signal quantification, which limit the practicality in resource-limited sites. Here we provide a visual detection of lead ions based on nanoparticle-amplified magnetophoresis and Mie scattering. Lead ions first react with GR-5 DNAzyme to release a DNA fragment that can connect magnetic microparticles (MMPs) and gold nanoparticles (AuNPs) through DNA hybridization. Next, the connected AuNPs are collected by magnetic separation and then released. Benefit from the hundreds of oligonucleotides on the AuNPs, tiny amount of AuNPs, which represent low concentration of lead ions, can effectively connect a second pair of MMPs and polystyrene microparticles (PMPs). Upon magnetophoresis, it changes solution turbidity from milky to clear because of the reduction of Mie scattering when less free PMPs suspend in the solution. Our results achieved a limit of detection (LOD) at 55 pM in 100 µl (reaction concentration) and 1.108 nM in 5 µl (sample concentration), which is much lower than the prescribed level in drinking water suggested by Environmental Protection Agency (72 nM). In addition, it also achieves high selectivity against other metal ions (> 50,000 to 1) and is compatible with detection in tap water, providing a visual, sensitive detection without complicated instrument.

1. Introduction

Environmentally hazardous substances in food [1,2] or water [3,4] pose significant threats to human health. Lead is one of the most lethal contaminants in industrial waste and drinking water. Because it is non-biodegradable, lead poisoning can accumulate in the human body, leading to prolonged impairment of brain function or fetus fatality during pregnancy [5]. Thus, to better control this problem, sensitive and quantitative detection of lead contamination is highly desired.

DNAzyme, a form of DNA oligonucleotides which could catalyze a specific hydrolytic cleavage in the presence of specific metal ions [6–10], has been employed as a primary agent for lead ion detection because it can be easily synthesized and is stable compared to protein-based enzymes or ribozymes. Many detection methods of lead ions have been built around GR-5 DNAzyme (GR-5) [11–19] because of its exceptional selectivity against other competing metal ions [20–22]. In the presence of lead ions, the DNAzyme is activated and cleaved at the RNA site (rA) of the substrate strand. Through such conformational change, DNAzyme with functional label can generate signals such as fluorescence [11,14–16,23–25], electrochemistry [17,26,27] and chemiluminescence [18,19]. However, those detections require expert techniques or complicated instruments for signal analysis. In contrast, visual detections can provide a simple and visible readout suitable for the general public. For example, based on the unique optical properties and high surface-to-volume ratio, gold nanoparticles (AuNPs) [28] have been employed to generate visual signals for lead detections [11,18,26,28–35]. Nevertheless, visual detection such as colorimetric assay is generally based on AuNP aggregation [29,30,32,33,35], which requires not only specific temperature control [29,30] but also large amounts of linkers to induce sufficient aggregation [33,35]. Thus, sufficient sensitivity is difficult to achieve.

Instead of directly using AuNP for signal generation, AuNPs can also be used as a trigger to initiate a subsequent reaction or process [31,32,34]. Adopting this idea, here we report a 2-step visual detection based on GR-5 with nanoparticle-amplified magnetophoresis and Mie scattering (Scheme 1). In the step 1, GR-5 is cleavable by lead ions and releases a DNA fragment that can connect magnetic microparticles (MMPs) and AuNPs through DNA hybridization (Fig. S1). The

* Corresponding author.
E-mail address: thchen@cityu.edu.hk (T.-H. Chen).

https://doi.org/10.1016/j.snb.2019.127564
Received 23 September 2019; Received in revised form 7 December 2019; Accepted 9 December 2019
Available online 16 December 2019
0925-4005/

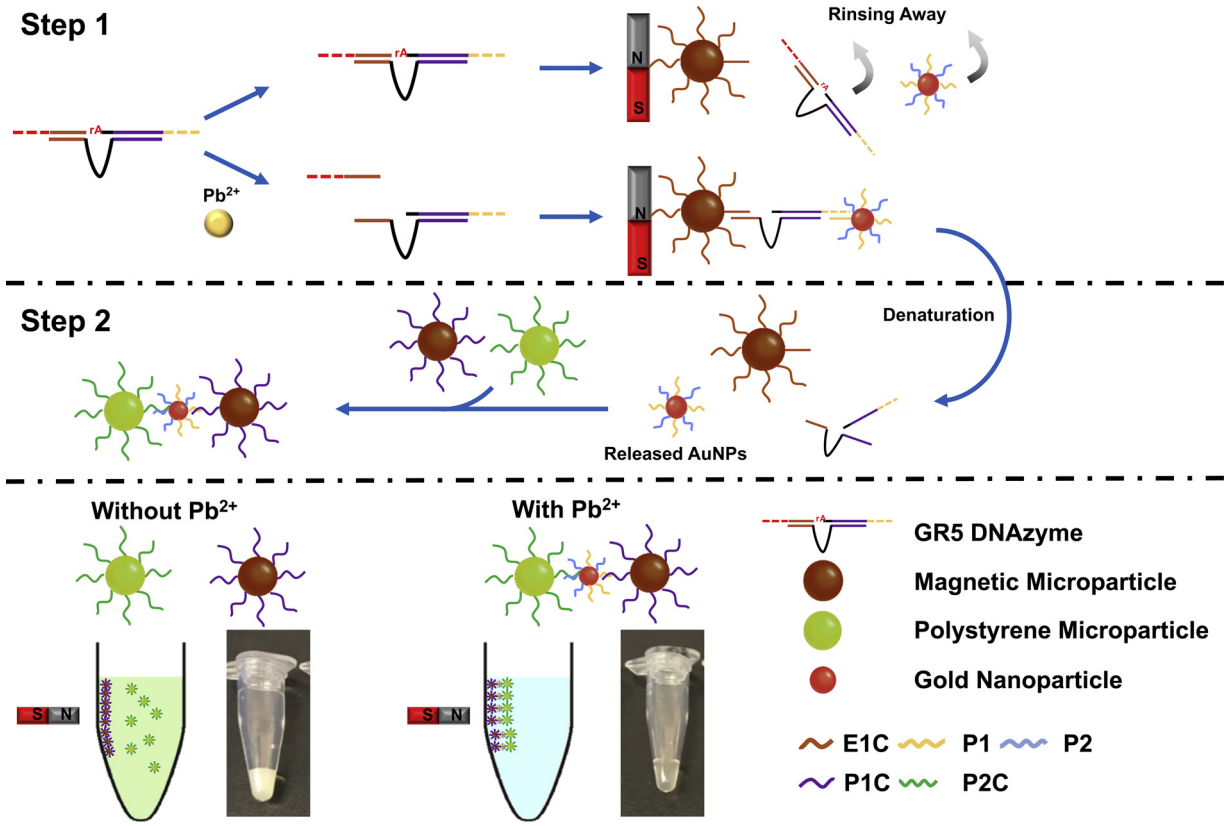

Scheme 1. Working principle of the visual detection of lead ions. [Step 1]: GR-5 DNAzyme is cleavable by lead ions and releases a fragment that can connect magnetic microparticles (MMPs) and gold nanoparticles (AuNPs). [Step 2]: After magnetic separation, the connected AuNPs are released by denaturation and then used to connect a second pair of MMPs and polystyrene microparticles (PMPs). [Final measurement]: Change of solution turbidity because of the reduced Mie scattering when less PMPs freely suspend in the solution.

connected AuNPs, with a number proportional to the amount of lead ions, can be collected by magnetic separation. In the step 2, the collected AuNPs are released by denaturation. Based on the vast amount of oligonucleotides on the released AuNPs, AuNPs can effectively hybridize to the oligonucleotides on the second pair of MMPs and polystyrene microparticles (PMPs), leading to the formation of MMPs-AuNPs-PMPs even with very tiny amount of AuNPs. After magnetic attraction, the solution turbidity changes from milky to clear because of the reduced Mie scattering when less PMPs freely suspend in the solution. Such two-step amplification achieved a limit of detection (LOD) at 55 pM in 100 μl (reaction concentration) and 1.108 nM in 5 μl (sample concentration), which is significantly lower than the prescribed level in drinking water suggested by Environmental Protection Agency (72 nM), and is extremely selective on lead ions against other metal ions (> 50,000 times), and applicable to detection in tap water. Overall, combining nanoparticle-amplified magnetophoresis and Mie scattering, we demonstrate a visual and sensitive detection of lead contamination without complicated instrument for signal analysis.

2. Experimental

2.1. Oligonucleotide sequence

The sequences of oligonucleotides are listed in Table S1. The GRDS (Integrated DNA Technologies) and GRE (BGI BIO-Solutions HONGKONG Co., Ltd.) were designed based on the original form [20] with extension on its two termini. Other oligonucleotides were synthesized from BGI BIO-Solutions HONGKONG Co., Ltd.. Once receiving, the oligonucleotides were dissolved in DEPC-treated water (Thermo Fisher Scientific). The P1's sequence was designed to hybridize with the 3′ end of GRDS, and is complementary to P1C. The E1C was designed to hybridize with the 3′ end of GRE, which is only revealed after hydrolytic cleavage of GR-5. Thus, once the GR-5 is cleaved (Fig. S1), the DNA fragment composed of 3′ end of cleaved GRDS and 3′ end of GRE can hybridize with P1 on AuNPs (15 nm in diameter; PERSer Nanotechnology Ltd.) and E1C on MMPs (CM01 N, 0.86 μm in diameter; 1.864×10^{10} particles/ml, Bangs Laboratories, Inc.), allowing AuNPs being connected to MMPs in the step 1. Note that the AuNPs were simultaneously modified with P2, which has sequence complementary to P2C. Thus, in the step 2, P1 and P2 on AuNPs can hybridize to P1C on MMPs and P2C on PMPs (CP01 F, 0.989 μm in diameter; 1.827×10^{10} particles/ml, Bangs Laboratories, Inc.). SGRDS target is a short single-strand DNA oligonucleotide that can hybridize with G' and P2 in juxtaposition. It was used to optimize the ratio between MMPs modified with G' and AuNPs modified with P1 and P2, or PMPs modified with P2. For immobilization on micro or nanoparticles, the oligonucleotides were either thiolated for binding to AuNPs (lengthened with poly T tail to enhance the hybridization efficiency) or biotinylated for binding to MMPs or PMPs coated with streptavidin. All hybridization of DNA oligonucleotides modified on particles was conducted at 25 ℃ for 30 min.

2.2. Modification of particles

The thiolated oligonucleotides P1 and P2 (6.25 μl, 100 μM) were first activated by (2-carboxyethyl) phosphine (TCEP, Sangon Biotech Ltd., 10 mM, 5 μl) for 1 h, and then mixed with 750 μl of AuNP solution (15 nm in diameter, particles/ml: 2.0×10^{10}) for overnight incubation. A step-wise aging process was conducted until 0.3 M NaCl was achieved, i.e. addition of 0.025 M NaCl (J&K Scientific) by 4 times, followed by 4 times of addition of 0.05 M NaCl, with 45 min time interval between each addition. After aging for 16 h, the AuNPs were

washed by centrifugation at 13.3 × g for 3 times with 30 min time interval each, followed by resuspension in 750 µl of TA buffer (50 mM Tris Acetate consisting of Tris(hydroxymethyl) aminomethane (J&K Scientific) and acetic acid (J&K Scientific), 0.2 M NaCl (J&K Scientific), and 0.2 % Tween 20 (Thermo Fisher Scientific)). The biotinylated oligonucleotides E1C, P1, P1C and P2C were immobilized onto MMPs or PMPs through 'biotin-streptavidin' complex. Briefly, 0.72 µg oligonucleotide was mixed to each µl of either MMPs or PMPs solution, where the provided oligonucleotide was significantly greater than the total capacity of microparticles to ensure that all binding sites are fully loaded. After gentle shaking in room temperature for 30 min, the particles were rinsed three times by TA buffer to remove the excess oligonucleotides. Finally, the particles were resuspended at 10 mg/ml.

2.3. Optimization of ratio of MMPs to PMPs or AuNPs

Synthesized DNA (SGRDS target) was used as the target at 4 µM in 5 µl to connect MMPs to AuNPs or 1.76 µM in 2.5 µl to connect MMPs to PMPs. Varied volume of MMPs modified with G' (1.25 µl, 2.5 µl, 3.75 µl, 5 µl, and 6.25 µl, 10 mg/mL) were used to connect to a fixed amount of AuNPs modified with P1 and P2 strand (80 µl, particles/ml: 2.0×10^{10}). The final volume was adjusted to 100 µl by TA buffer. Similarly, the varied volume of MMPs modified with G' (0.5 µl, 1 µl, 2 µl, 3.5 µl, 5 µl, and 7.5 µl, 10 mg/mL) were used to connect to a fixed amount of PMPs modified with P2 strand (3.5 µl, 10 mg/mL). The experimental solution was brought to 22 µl by adding TA buffer. After hybridization, the absorbance of the supernatant was measured at the wavelength of 400 nm by UV–vis spectrometer (BioDrop µlITE, UK) for PMPs; or at the wavelength of 520 nm by Agilent 8453 spectrophotometer (UV-AG-1) for AuNPs.

2.4. Hydrolytic reaction of GR-5 by lead ion

GRDS and GRE were hybridized at a 1:1 ratio for 30 min at 25 ℃ to form the GR-5 DNAzyme at 1 µM in 30 µl in the TA buffer. Because a small amount of GR-5 may be unexpectedly cleaved during GR-5 formation, 50 µl MMPs with E1C (10 mg/ml) were added to remove the cleaved fragment. To determine the LOD, 5 µl of different concentrations of lead (II) acetate trihydrate (from J&K Scientific) was prepared in TA buffer. For selectivity test, various metal ions including Nickel (Ni), Copper (Cu), Cadmium (Cd), Calcium (Ca), Barium (Ba) and Mercury (Hg) (all are in AA standard form from J&K Scientific) were used to react with GR-5 at concentration of 1 mM diluted in TA buffer in 5 µl. For the reaction in different pH values, 5 µl DEPC-treated water with various concentrations of lead ions was first adjusted by the addition of NaOH or HCl until the pH reached 3, 6, 9, or 11. For tests in tap water, lead ions with different concentrations was spiked in tap water, and the final volume was 5 µl. Next, the lead solution reacted with the purified GR-5 at 100 nM in 10 µl for 45 min. Of note, we found that the use of bovine serum albumin (BSA) coating in microcentrifuge would inhibit the hydrolytic reaction between GR-5 and lead ions (lane 5–6 in Fig. S2). Such inhibition may be due to the binding between lead ions and BSA [36,37]. Hence, BSA-coated tubes were not used in the reaction between GR-5 and lead ions.

2.5. Hybridization between MMPs and PMPs using cleaved GR-5

The GR-5 solution after reaction with lead ions was added into 3.5 µl of MMPs (10 mg/mL) modified with E1C in microcentrifuge tube coated with BSA (1 %). After 30 min of shaking, three times washing by TA buffer on a magnetic rack was conducted to remove the excess oligonucleotides, leaving only cleaved GR-5 fragment connected to the MMPs. Next, 3.5 µl of PMPs (10 mg/mL) modified with P1 was mixed into the solution and incubated for 30 min with gentle vortex at room temperature. Supernatant with free PMPs was then collected in microcentrifuge tube coated with BSA (1 %) by magnetic separation for direct visual inspection or quantitatively analysis by optical absorbance at the wavelength of 400 nm by UV–vis spectrometer (BioDrop µLITE, UK).

2.6. Hybridization between MMPs and AuNPs using cleaved GR-5

The GR-5 solution after reaction with lead ions was added into 5 µl of MMPs (10 mg/mL) modified with E1C in microcentrifuge tube coated with BSA (1 %). After 30 min with shaking, the supernatant was removed using magnetic separation. After three times of washing by TA buffer, the MMPs linked with cleaved GR-5 were mixed with the AuNPs (15 nm in diameter, particles/ml: 2.0×10^{10}, 80 µl) modified with both P1 and P2 for 30 min. After magnetic separation, the supernatant was collected in microcentrifuge tube coated with BSA (1 %) for later use or measurement of absorbance at wavelength of 520 nm by Agilent 8453 spectrophotometer (UV-AG-1).

2.7. Amplified visual detection using collection of linked AuNPs

The linked MMPs and AuMPs were denatured using NaOH solution (10 µl, 1 M) for 5 min in microcentrifuge tube coated with BSA (1 %), allowing the isolation of AuNPs. The released AuNPs were rinsed twice using 100 µl, 0.1 M phosphate buffer (0.0754 M Na_2HPO_4, 0.0246 M NAH_2PO_4, pH 7.4) and concentrated in 10 µl of 0.1 M phosphate buffer. Next, 5 µl of MMPs (10 mg/ml) modified with P1C and 3.5, 7 or 8.75 µl of PMPs (10 mg/ml) modified with P2C were added for incubation inside the 0.1 M phosphate buffer for 1 h. For visual detection of MMPs-AuNPs-PMPs based on magnetophoretic effect, supernatant of free PMPs was collected in microcentrifuge tube coated with BSA (1 %) by magnetic separation for direct visual inspection or quantitatively analysis of optical absorption at the wavelength of 400 nm by UV–vis spectrometer (BioDrop µLITE, UK).

2.8. Agarose gel electrophoresis

Five percent agarose gel was formed by dissolving 5 g of agarose powder (Thermo Fisher Scientific) in 100 ml of 1X TAE buffer (diluted from 10X TAE buffer, Thermo Fisher Scientific). The solution was microwaved until boiling, and all the agarose particles were dissolved. Then, the solution was mixed with 3 µl, 10,000X gel red (BIOTIUM) and poured into the casting tray until it cooled down and formed the gel.

Hybridization of oligonucleotide (200 nM diluted by TA buffer) was conducted at room temperature for 1 h. Next, oligonucleotides (200 nM for each strand) were loaded in the gel for conducting DNA migration inside the gel tank (electrophoresis unit) prefilled with the 1X TAE buffer under 130 V for 45 min. The gel was visualized by BIO-RAD Gel Doc EZ Imager. Different-length strands can be observed to determine the efficiency of double-strands formation. GeneRuler Ultra Low Range DNA Ladder (SM1211, Thermo Fisher Scientific) was used as a reference.

2.9. Dynamic light scattering (DLS)

The MMPs, AuNPs, and PMPs were prepared in TA buffer with the volume of 25 µl (10 mg/ml), 400 µl (particles/ml: 2.0×10^{10}) and 35 µl (10 mg/ml) respectively. For MMPs-AuNPs-PMPs, solution was mixed with 25 µl MMPs, 400 µl AuNPs and 35 µl PMPs (same as the experimental ratio). All samples were centrifuged and resuspended in 450 µl of TA buffer and incubated at 25 ℃ for 30 min with shaking for hybridization between MMPs, AuNPs, and PMPs. Afterward, the measurement was conducted by Dynamic Light Scattering Particle Size Analyzer (Malvern Zetasizer Nano ZS) with the measured volume at 400 µl.

2.10. Transmission electron microscopy (TEM)

The MMPs, AuNPs, and PMPs were prepared in TA buffer with the volume of 6.25 μl (10 mg/ml), 100 μl (particles/ml: 2.0×10^{10}), and 8.75 μl (10 mg/ml), respectively. For MMPs-AuNPs-PMPs, solution was mixed with 6.25 μl MMPs, 100 μl AuNPs and 8.75 μl PMPs together. All samples were centrifuged and resuspended in 100 μl of TA buffer. Next, the solutions were concentrated 10 times in TA buffer by centrifugation and incubated at 25 ℃ for 30 min with shaking for hybridization between MMPs, AuNPs, and PMPs. Seven microliters of the concentrated solution was deposited on a 300 mesh copper grid, and allowed to absorb for 30 min. After that, excess solution was removed, followed by rinsing with ethanol and absorbed by filter paper. After being kept in a desiccator overnight, the TEM imaging was carried out using a Transmission Electron Microscope (FEI / Philips Tecnai 12 BioTWIN).

3. Results and discussion

3.1. Gel electrophoresis of hydrolytic cleaved GR-5

We first conducted gel electrophoresis to visualize the hydrolytic cleavage of GR-5. GR-5 can be successfully formed by hybridization between GRDS and GRE at a 1:1 ratio, while there was a slight amount of GR-5 auto-cleaved (lane 1–3 in Fig. 1). With the addition of lead ions (200 nM), the majority of GR-5 was cleaved (lane 4 in Fig. 1), releasing a fragment which can hybridize with P1 at 3′ end of GRDS and E1C at 3′ end of GRE (lane 5–7 in Fig. 1). Note that the reaction can occur at 25 ℃ or 37 ℃ (Fig. S3), suggesting the tolerance to temperature variation within the range of room temperature. Of note, the intact GR-5 can only bind with P1 but not E1C (lane 8–10 in Fig. 1) because the 3′ end of GRE is occupied by the intact GRDS. Based on such design, only cleaved GR-5 is allowed to bind to E1C and P1 simultaneously.

3.2. Visual detection using magnetophoresis and Mie scattering without amplification

Based on the enzymatic cleavage of GR-5, we next investigated the visual detection of lead ions without amplification. The principle is based on GR-5-mediated connection between MMPs and PMPs, i.e. MMPs-GR-5-PMPs (scheme in Fig. 2). We first optimized the ratio between MMPs to PMPs to ensure sufficient change of solution turbidity after forming the MMPs-GR-5-PMPs. For simplicity, we used synthesized single-strand DNA, i.e. SGRDS target (200 nM), to represent the cleaved GR-5 fragment for particle connections. Correspondingly, G' was modified on MMPs and P2 was modified on PMPs such that G' and P2 can hybridize with the SGRDS target in juxtaposition, leading to the connections between MMPs to PMPs that reduce the solution turbidity after magnetophoresis. To optimize the particle ratio, we changed the volume of MMP solution (10 mg/mL) while keeping the sufficient amount of PMPs fixed (3.5 μl, 10 mg/mL) such that high absorbance can be obtained when the target is absent. As shown in Fig. S4A, after mixing and magnetic attraction, the absorbance value was reduced with the increasing volume of MMPs due to the reduced Mie scattering when more MMPs were available to attract PMPs to the sidewall. Based on the situation of the lowest absorbance, which indicates the effective particle-particle connections, 3.5 μl of MMPs was chosen to connect PMPs.

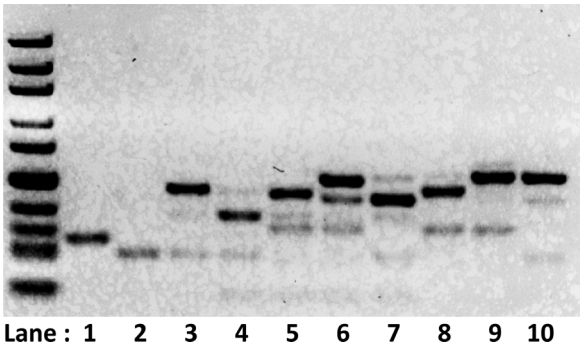

Fig. 1. Agarose gel analysis of GR-5 DNAzyme hybridization. Lane 1: GRDS, substrate strand; Lane 2: GRE, enzyme strand; Lane 3: GR-5; Lane 4: GR-5 + Pb^{2+} (200 nM); Lanes 5: GR-5 + Pb^{2+} (200 nM) + E1C; Lane 6: GR-5 + Pb^{2+} (200 nM) + E1C + P1; Lane 7: GR-5 + Pb^{2+} (200 nM) + P1; Lane 8: GR-5 + E1C; Lane 9: GR-5 + P1; Lane 10: GR-5 + E1C + P1.

With the optimized pair of MMPs to PMPs, we next investigated the suitable GR-5 concentration to differentiate samples with/without lead ions. Here, MMPs were modified with single-strand oligonucleotide E1C, while PMPs were modified with P1. As such, the fragment released from cleaved GR-5 can hybridize with E1C and P1 simultaneously, increasing the connection between MMPs to PMPs. We found that GR-5 of 1 or 5 nM was insufficient to connect MMPs and PMPs, while excess amount of GR-5 such as 25 or 50 nM would cause too much auto-cleaved GR-5 fragment that made the solution clear even when lead ion was absent (Fig. 2A). In contrast, when GR-5 was 10 nM, the increase of lead ion concentration led to an apparent reduction of absorbance, providing the best contrast between samples with/without lead ions (Fig. 2A).

With optimized GR-5 concentration and particle ratio, we next explored the LOD of this visual detection without amplification. When the concentration of lead ions increased from 4.4 nM to 880 nM, the absorbance of the PMPs solution reduced. Using the calibration graph plotted in the linear range of 0–80 nM (Fig. S5 and Fig. 2B), the LOD was estimated as 6.22 nM in 22 μl (reaction concentration) or 27.38 nM in 5 μl (sample concentration), which were calculated based on $3\ \sigma/m$ [10,38], where σ is the standard deviation of blank sample (0.05412), and m is the absolute slope of the calibration equation (0.00593).

3.3. Visual detection using nanoparticle-amplified magnetophoresis and Mie scattering

To enhance the detection sensitivity, we next applied the nanoparticle-based amplification (Scheme 1). Instead of using GR-5 for direct connection between MMPs and PMPs, MMPs first connected to AuNPs by cleaved GR-5 fragment such that the number of connected AuNPs is proportional to the amount of lead ions. After the magnetic separation, the AuNPs can be released from the MMPs through DNA denaturation. Simultaneously carrying P1 and P2 with a great number, the AuNPs can be used to connect a second pair of MMPs modified with P1C and PMPs modified with P2C, leading to strengthened connection between MMPs and PMPs, i.e. MMPs-AuNPs-PMPs. We first used DLS and TEM to characterize the particle connections. The result of DLS showed that the diameter of MMPs and PMPs is 0.999 ± 0.447 μm and 1.087 ± 0.224 μm, respectively, while the diameter of AuNPs is 29.48 ± 18.35 nm (Fig. S6). After hybridization, the diameter of MMPs-AuNPs-PMPs becomes 2.157 ± 1.04 μm, suggesting the successful connection between the three particles. Furthermore, using TEM for direct observation, it is clear the formation of MMPs-AuNPs-PMPs is mediated by AuNPs that connect MMPs and PMPs (Fig. S7).

We next optimized the ratio between MMPs and AuNPs in the step1 using SGRDS target (200 nM) to represent the cleaved GR-5 fragment. Similar to the optimization of particle ratio above, we adjusted the volume of MMPs (10 mg/mL) when AuNP concentration was fixed at a sufficient concentration (particles/ml: 2.0×10^{10}, 80 μl) to ensure high absorbance when SGRDS target is absent. According to the results, 5 μl of MMPs was chosen to connect AuNPs (Fig. S4B). Next, we optimized the amount of PMPs to be used in the step 2. When the lead ion was absent, a very small amount of AuNPs, i.e. due to non-specific binding or auto-cleaved GR-5, can be still collected by magnetic separation, even though most of the auto-cleaved GR-5 was already removed by MMPs with E1C before the lead ion reaction. Because these AuNPs still carry strong connectivity, they can still greatly reduce the number of

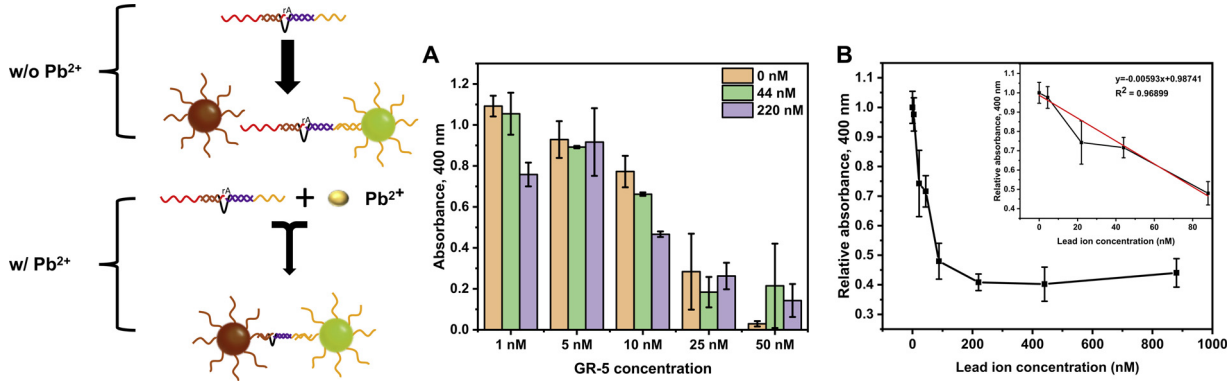

Fig. 2. Visual detection using magnetophoresis and Mie scattering without amplification. (A) Optimization of GR-5 DNAzyme concentration for connection of MMPs-GR-5-PMPs (mean ± max deviation, n = 3). (B) Linear range of the relative absorbance at wavelength of 400 nm with respect to the concentration of lead ions (mean ± max deviation, n = 3). Inlet: line fitting within the lineage range of the relative absorbance with respect to the concentration of lead ions.

free PMPs in the step 2, causing the increased background noise or false positive signals. To compensate it, we adopted more PMPs in the step 2 after amplification. PMPs of 3.5, 7 and 8.75 µl were tested with the negative control and sample solution with lead ion solution (20 nM in 5 µl). When PMPs is 3.5 µl, we found that the absorbance value of sample with or without lead ion was below 0.25, indicating that almost all PMPs were linked to MMPs through the AuNPs (Fig. S8). In contrast, by increasing the volume of PMPs, we found that 7 µl and 8.75 µl of PMPs used in the amplification step not only reduced the noise but also increase the signal-to-noise ratio. Consequently, 7 µl PMPs were applied in the step 2.

After applying the amplification with the optimized particle ratio, we again observed a reduction of Mie scattering when lead concentration increased (Fig. 3A-C). By plotting the calibration graph with a linear range of 0–1 nM (Fig. 3D), the LOD achieved to 55 pM in 100 µl (reaction concentration) or 1.108 nM in 5 µl (sample concentration), which were calculated based on 3 σ/m, where σ as 0.13434 and m as 0.36373. Thus, comparing to the LOD without amplification (Fig. 2B), the signal was amplified to around 25 times. By comparing to other state-of-the-art detections (Table S2), our method achieved high sensitivity comparable or even better than most of the methods based on fluorescence or colorimetric signals, providing a sensitive and visual detection of lead contamination without complicated instrument.

3.4. Selectivity

To validate the selectivity of this amplified visual detection, we conducted a test with different metal ions that may be present in natural or industrial water source such as calcium (Ca) mercury (Hg), cadmium (Cd) and copper (Cu), or may accompany with lead as a binary product such as nickel (Ni) [5,39] and barium (Ba) [40]. Remarkably, our detection is highly selective toward lead ions (20 and 200 nM) than any other metal ions with much higher concentration (1 mM) (Fig. 4). Based on the concentration of use, the selectivity is at least 50,000–1. Therefore, it is feasible to apply our method for the detection of real water samples even if other metal ions are present.

3.5. Detection in different acidic/basic environment

To investigate the compatibility of this assay in different environment, we used lead ion samples spiked in water with pH = 3, 6, 9 and 11, which represents the acidic or basic condition such as the surface water systems (pH = 6.5–8.5), the groundwater system (pH = 6–8.5) and extreme condition which may not be even suitable for drinking (pH = 3 or 11). The result showed that, while the signal-to-noise ratio was reduced, we can still differentiate sample with lead ion > 20 nM in mildly acidic/basic condition (pH = 6 and 9), and sample with lead

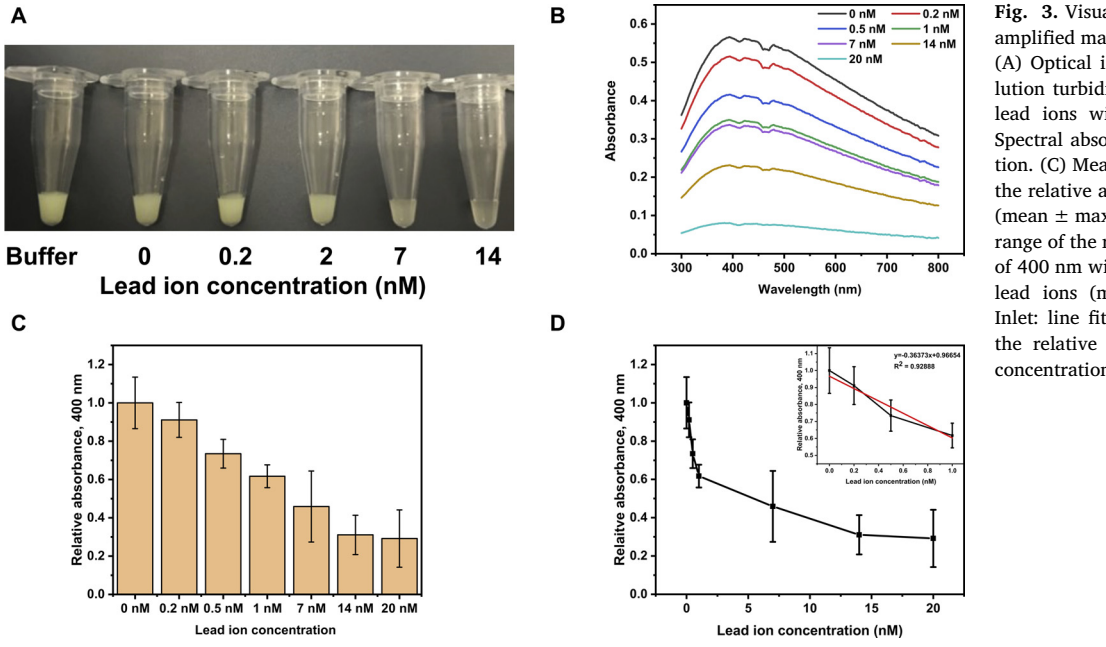

Fig. 3. Visual detection using nanoparticle-amplified magnetophoresis and Mie scattering. (A) Optical image showing the change of solution turbidity resulted from the presence of lead ions with different concentrations. (B) Spectral absorbance measurement of the solution. (C) Measurement of solution turbidity by the relative absorbance at 400 nm wavelength (mean ± max deviation, n = 3). (D) Linear range of the relative absorbance at wavelength of 400 nm with respect to the concentration of lead ions (mean ± max deviation, n = 3). Inlet: line fitting within the lineage range of the relative absorbance with respect to the concentration of lead ion.

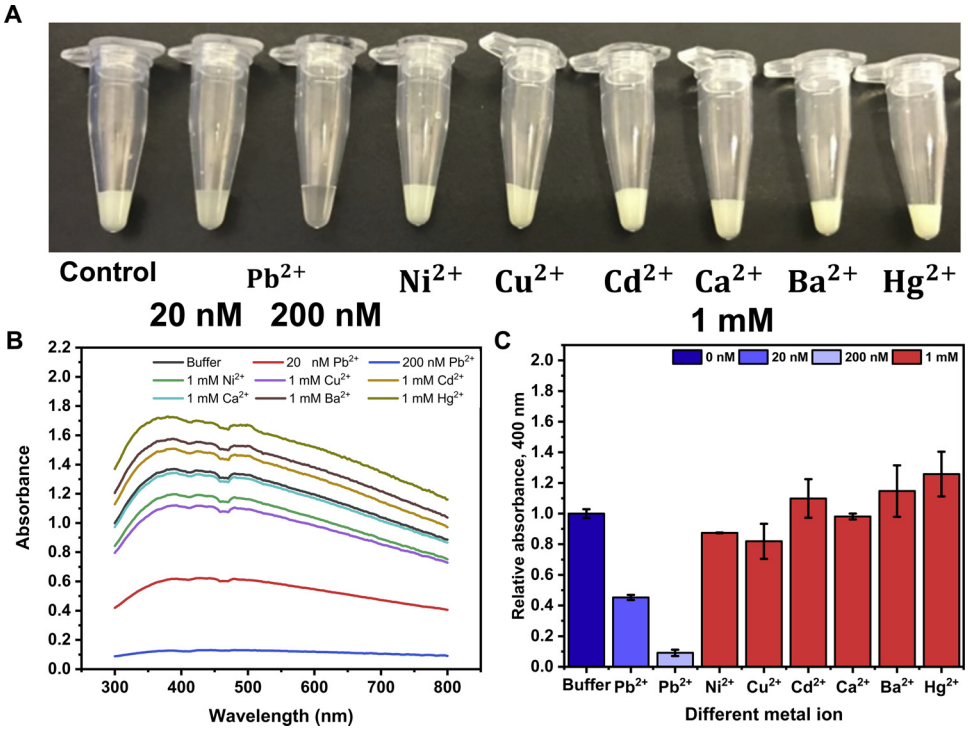

Fig. 4. Selectivity of lead detection against other six metal ions with higher concentration (1 mM). (A) Optical image showing the change of solution turbidity resulted from the presence of different metal ions. (B) Spectral absorbance measurement of solution. (C) Measurement of solution turbidity by the relative absorbance at 400 nm wavelength (mean ± max deviation, n = 3).

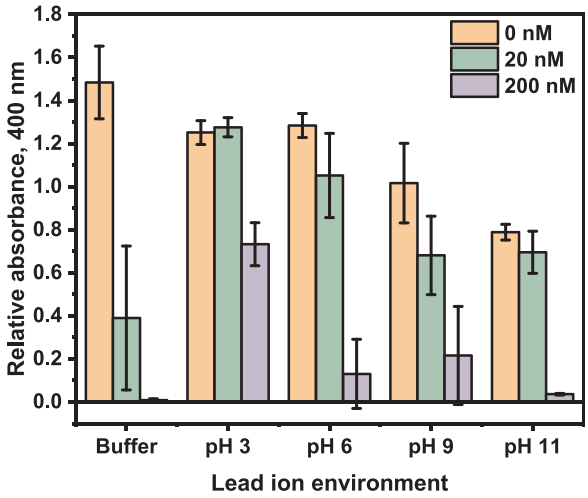

Fig. 5. Measurement of solution turbidity by the relative absorbance at 400 nm wavelength showing the lead ion detection in acidic/basic environment (mean ± max deviation, n = 3).

ion > 200 nM in extremely acidic/basic condition (pH = 3 and 11) (Fig. S9 and Fig. 5). Thus, while the extremely acidic/basic environment may affect the detection mechanism by reducing the stability of DNA hybridization, our detection still works in a mildly acidic/basic environment, which is still sufficient for monitoring the safety of drinking water.

3.6. Detection in tap water

At last, to validate the compatibility and practicability of our assay towards real applications, we applied this assay for detection in tap water. Lead ions were spiked into the tap water (final concentration: 10, 20, or 100 nM), and the results were compared to that in buffer solution as a reference. We found that the water sample without adding lead already led to a small reduction of absorbance value, suggesting that lead ions were contained in the tap water (Fig. 6). Based on the calibration curve (Fig. 3D), we can determine the concentration of lead in tap water is 0.359 nM in 5 μl (sample concentration). Next, by spiking additional lead ions into such tap water sample, the additional lead ion of 10 nM can cause a reduction of absorbance value similar to the 20 nM case in buffer, and achieved almost zero absorbance for the case with an additional lead ion of 20 nM (Fig. 6). Together, the results show the compatibility of our assay for practical application in tap water sample and suggest the presence of lead contamination in tap water in Hong Kong.

4. Conclusion

Lead poisoning in drinking water poses severe risk to human health. By combining nanoparticle-amplified magnetophoresis and Mie scattering, we demonstrate a visual detection of lead with LOD of 55 pM in 100 μl (reaction concentration) and 1.108 nM in 5 μl (sample concentration)), which is much lower than the prescribed level in drinking water suggested by Environmental Protection Agency (72 nM). Also, it achieves high selectivity (> 50,000–1) against other competing metal ions. More importantly, this method is compatible with detection in tap water or environmental sample with mild acidity/basicity, suggesting that this simple and highly sensitive detection as a potential application for monitoring lead contamination in drinking water.

Declaration of Competing Interest

The authors declare no competing financial interest.

Acknowledgments

We are pleased to acknowledge the funding support from the Early Career Scheme (project no. 21214815), General Research Fund (project nos. 11277516 and 11217217), and NSFC/RGC Joint Research Scheme (N_CityU119/19) from the Hong Kong Research Grant Council, and internal grants from City University of Hong Kong (9667161 and 6000632).

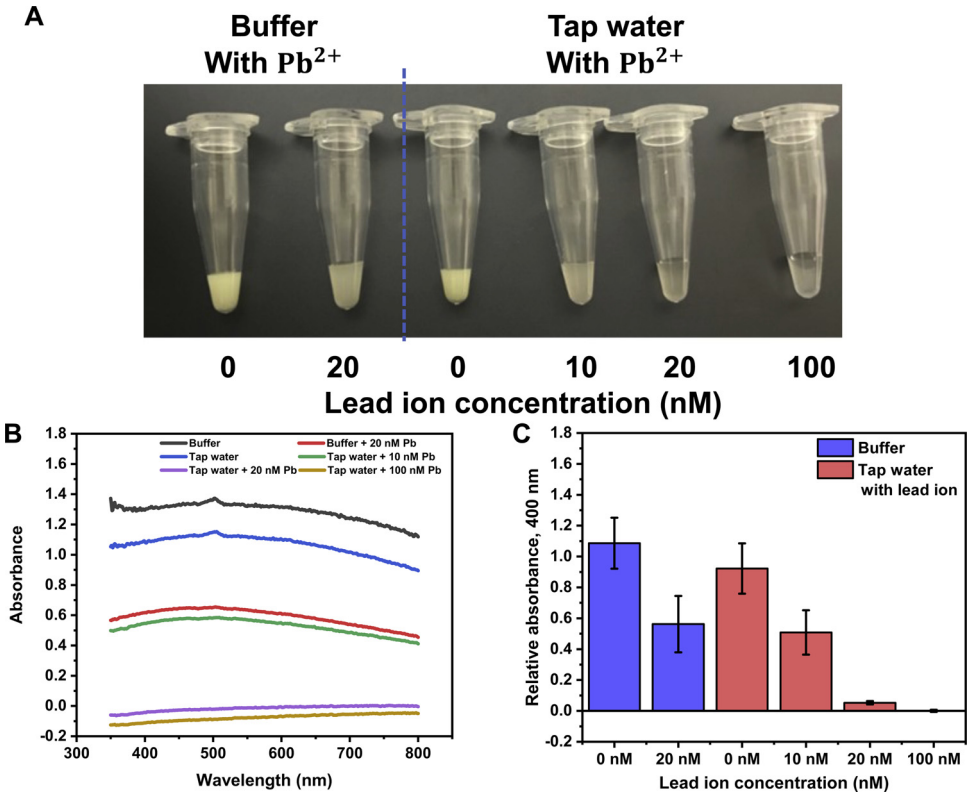

Fig. 6. Lead ion detection in buffer and tap water. (A) Optical image showing the change of solution turbidity resulted from the presence of lead ions. (B) Spectral absorbance measurement of solution. (C) Measurement of solution turbidity by the relative absorbance at 400 nm wavelength (mean ± max deviation, n = 3).

Appendix A. Supplementary data

Supplementary material related to this article can be found, in the online version, at doi:https://doi.org/10.1016/j.snb.2019.127564.

References

[1] L. Wang, et al., Rapid and visual detection of aflatoxin B1 in foodstuffs using aptamer/G-quadruplex DNAzyme probe with low background noise, Food Chem. 271 (2019) 581–587.

[2] C. Yang, et al., Aptamer-DNAzyme hairpins for biosensing of Ochratoxin A, Biosens. Bioelectron. 32 (1) (2012) 208–212.

[3] Z. Li, et al., An aptamer-based fluorescent sensor array for rapid detection of cyanotoxins on a smartphone, Anal. Chem. (2019).

[4] S.J. Xiao, et al., Highly sensitive DNAzyme sensor for selective detection of trace uranium in ore and natural water samples, Sens. Actuators B Chem. 210 (2015) 656–660.

[5] L. Patrick, Lead toxicity, a review of the literature. Part I: exposure, evaluation, and treatment, Altern. Med. Rev. 11 (1) (2006).

[6] Y. Zhou, et al., Current progress in biosensors for heavy metal ions based on DNAzymes/DNA molecules functionalized nanostructures, A Review Sens. Actuators B: Chem. 223 (2016) 280–294.

[7] R. Saran, J. Liu, A silver DNAzyme, Anal. Chem. 88 (7) (2016) 4014–4020.

[8] H. Wang, Y. Liu, G. Liu, Label-free biosensor using a silver specific RNA-Cleaving DNAzyme functionalized single-walled carbon nanotube for silver ion determination, Nanomaterials 8 (4) (2018) 258.

[9] J. Liu, Y. Lu, A DNAzyme catalytic beacon sensor for paramagnetic Cu2+ ions in aqueous solution with high sensitivity and selectivity, J. Am. Chem. Soc. 129 (32) (2007) 9838–9839.

[10] Y. Chen, et al., DNAzyme-based biosensor for Cu2+ ion by combining hybridization chain reaction with fluorescence resonance energy transfer technique, Talanta 155 (2016) 245–249.

[11] H.-B. Wang, et al., A highly sensitive and selective biosensing strategy for the detection of Pb 2+ ions based on GR-5 DNAzyme functionalized AuNPs, New J. Chem. 37 (8) (2013) 2557–2563.

[12] W. Deng, et al., Electrochemiluminescence-based detection method of lead(II) ion via dual enhancement of intermolecular and intramolecular co-reaction, Analyst 140 (12) (2015) 4206–4211.

[13] H.B. Teh, H. Li, S.F.Y. Li, Highly sensitive and selective detection of Pb2+ ions using a novel and simple DNAzyme-based quartz crystal microbalance with dissipation biosensor, Analyst 139 (20) (2014) 5170–5175.

[14] A. Ravikumar, P. Panneerselvam, K. Radhakrishnan, Fluorometric determination of lead(II) and mercury(II) based on their interaction with a complex formed between graphene oxide and a DNAzyme, Microchim. Ichnoanal. Acta 185 (1) (2018) 2.

[15] D. Zhang, et al., Nanoparticles-free fluorescence anisotropy amplification assay for detection of RNA nucleotide-cleaving DNAzyme activity, Anal. Chem. 87 (9) (2015) 4903–4909.

[16] T. Fu, et al., A label-free DNAzyme fluorescence biosensor for amplified detection of Pb2+-based on cleavage-induced G-quadruplex formation, Talanta 147 (2016) 302–306.

[17] H. Cui, et al., A novel impedimetric biosensor for detection of lead (II) with low-cost interdigitated electrodes made on PCB, Electroanalysis 28 (9) (2016) 2000–2006.

[18] Y. Zhang, et al., Electrochemiluminescence of graphitic carbon nitride and its application in ultrasensitive detection of lead(II) ions, Anal. Bioanal. Chem. 408 (25) (2016) 7181–7191.

[19] A. Gao, et al., Electrochemiluminescent lead biosensor based on GR-5 lead-dependent DNAzyme for Ru (phen) 3 2+ intercalation and lead recognition, Analyst 138 (1) (2013) 263–268.

[20] T. Lan, K. Furuya, Y. Lu, A highly selective lead sensor based on a classic lead DNAzyme, Chem. Commun. 46 (22) (2010) 3896–3898.

[21] P.-J.J. Huang, J. Liu, Two Pb 2+-specific dnazymes with opposite trends in split-site-dependent activity, Chem. Commun. 50 (34) (2014) 4442–4444.

[22] R. Saran, J. Liu, A comparison of two classic Pb 2+-dependent RNA-cleaving DNAzymes, Inorg. Chem. Front. 3 (4) (2016) 494–501.

[23] X.-H. Zhao, et al., Graphene–DNAzyme based biosensor for amplified fluorescence "turn-on" detection of Pb2+ with a high selectivity, Anal. Chem. 83 (13) (2011) 5062–5066.

[24] X. Li, et al., A "turn-on" fluorescent sensor for detection of Pb 2+ based on graphene oxide and G-quadruplex DNA, J. Chem. Soc. Faraday Trans. 15 (31) (2013) 12800–12804.

[25] S. Pang, S. Liu, X. Su, An ultrasensitive sensing strategy for the detection of lead (II) ions based on the intermolecular G-quadruplex and graphene oxide, Sens. Actuators B Chem. 208 (2015) 415–420.

[26] Y. Wang, J. Irudayaraj, A SERS DNAzyme biosensor for lead ion detection, Chem. Commun. 47 (15) (2011) 4394–4396.

[27] Y. Xiao, A.A. Rowe, K.W. Plaxco, Electrochemical detection of parts-per-billion lead via an electrode-bound DNAzyme assembly, J. Am. Chem. Soc. 129 (2) (2007) 262–263.

[28] Z. Wang, J.H. Lee, Y. Lu, Label-free colorimetric detection of lead ions with a nanomolar detection limit and tunable dynamic range by using gold nanoparticles and DNAzyme, Adv. Mater. 20 (17) (2008) 3263–3267.

[29] J. Liu, Y. Lu, A colorimetric lead biosensor using DNAzyme-directed assembly of gold nanoparticles, J. Am. Chem. Soc. 125 (22) (2003) 6642–6643.

[30] J. Liu, Y. Lu, Accelerated color change of gold nanoparticles assembled by DNAzymes for simple and fast colorimetric Pb2+ detection, J. Am. Chem. Soc. 126 (39) (2004) 12298–12305.

[31] S. Chen, et al., Enzyme-free amplification by nano sticky balls for visual detection of ssDNA/RNA oligonucleotides, ACS Appl. Mater. Interfaces 7 (41) (2015) 22821–22830.
[32] B. Chen, et al., Scanometric nanomolar lead (II) detection using DNA-functionalized gold nanoparticles and silver stain enhancement, Sens. Actuators B Chem. 200 (2014) 310–316.
[33] S. Thatai, et al., Trace colorimetric detection of Pb2+ using plasmonic gold nanoparticles and silica–gold nanocomposites, Microchem. J. 124 (2016) 104–110.
[34] Y. Huang, et al., Target-responsive DNAzyme cross-linked hydrogel for visual quantitative detection of lead, Anal. Chem. 86 (22) (2014) 11434–11439.
[35] P. Chen, et al., Colorimetric detection of lead ion based on gold nanoparticles and lead-stabilized G-quartet formation, J. Biomed. Sci. Eng. 8 (7) (2015) 451.
[36] A. Belatik, et al., Locating the binding sites of Pb (II) ion with human and bovine serum albumins, PLoS One 7 (5) (2012) e36723.
[37] L. Peng, et al., Calorimetric study of nonspecific interaction between lead ions and bovine serum albumin, Biol. Trace Elem. Res. 118 (2) (2007) 97–103.
[38] A. Shrivastava, V.B. Gupta, Methods for the determination of limit of detection and limit of quantitation of the analytical methods, Chron. Young Sci. 2 (1) (2011) 21.
[39] P. Franke, D. Neuschütz, Ni-Pb (nickel - lead), in binary systems, in: P. Franke, D. Neuschütz (Eds.), Part 5: Binary Systems Supplement 1: Phase Diagrams, Phase Transition Data, Integral and Partial Quantities of Alloys, Springer Berlin Heidelberg, Berlin, Heidelberg, 2007, pp. 1–3.
[40] B. Predel, B-Ba – C-Zr, O. Madelung (Eds.), Ba-Pb (Barium-Lead), Springer Berlin Heidelberg, Berlin, Heidelberg, 1992, pp. 1–2.

Lok Ting Chu received her B.Sc. degree in Bioengineering from City University of Hong Kong. She then joined Dr. Chen's research group in City University of Hong Kong as a fulltime Ph.D. candidate. Her research interest focuses on development of nucleic acid based biosensors and selective gene silencing in live cells.

Hoi Man Leung received her B.Sc. degree in Chemistry from City University of Hong Kong in 2017. She then joined Dr. Lo's research group as a fulltime Ph.D. candidate. Her research interests focus on the development of functional DNA- and nanoparticle-based materials for biomedical applications.

Pik Kwan Lo received her B.S. and M.Phil. in Chemistry from Hong Kong Baptist University in 2004 and 2006. She obtained her Ph.D. degree from McGill University in 2010 under the supervision of Professor Hanadi F. Sleiman. After that she moved to Harvard University for her postdoctoral research. She is currently an Associate Professor in the Department of Chemistry at City University of Hong Kong. Her research interests include design and assembly of bio-inspired DNA-based nanostructures and synthesis of advanced nanomaterials for biomedical applications.

Ting-Hsuan Chen received his B.S. degree (2003) and M.S. degree (2005) in National Tsing Hua University, Taiwan, and obtained his Ph.D. degree in Mechanical Engineering at University of California, Los Angeles, USA (2012). He is currently an Associate Professor in Biomedical Engineering at City University of Hong Kong, Hong Kong Special Administrative Region. His research interest is leveraging the microtechnology for measurement of cell chiral mechanics and development of DNA nanosensors to detect biomarkers in live cells or visual assays for point-of-care applications